Rough Terrain Reconstruction for Rover Motion Planning

David Gingras, Tom Lamarche, Érick Dupuis
Space Exploration
Canadian Space Agency

Jean-Luc Bedwani
Robotics and Civil
Research Institute of Hydro-Quebec

The Seventh Canadian Conference on Robotics and Computer Vision
Ottawa, Canada
June 1st 2010

Outline

Terrain Measurement

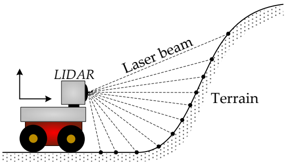

(a) Context of measurement

(b) Raw point cloud

FIG.: Terrain measurement using a LIDAR sensor

Terrain Measurement

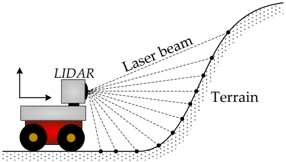

(a) Context of measurement

(b) Raw point cloud

FIG.: Terrain measurement using a LIDAR sensor

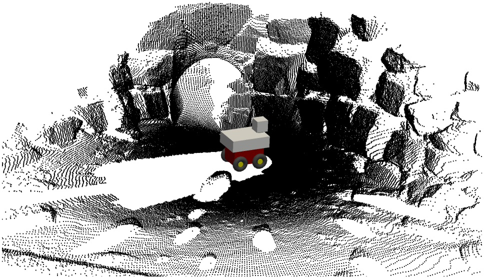

FIG.: 3D point cloud collected in the field (155 000 pts)

Terrain Reconstruction

Objective

Reconstruction of a terrain surface from a sparse 3D point cloud collected using the LIDAR sensor.

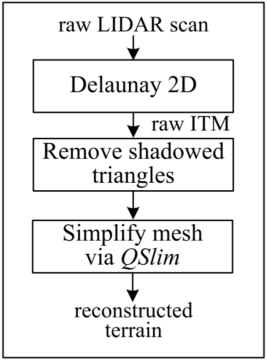

FIG.: Flow diagramm of the surface reconstruction process

Terrain Reconstruction

A triangulation is built using the Delaunay algorithm applied to the raw LIDAR scan expressed in polar coordinates. The vertices are then converted to a cartesian frame.

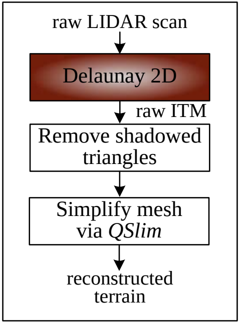

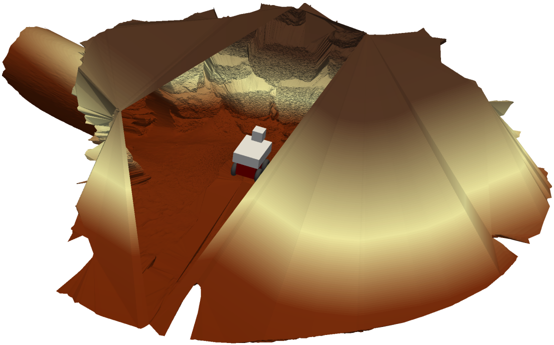

FIG.: Raw Irregular Triangular Mesh (ITM)

Terrain Reconstruction

Because Delaunay algorithm always returns a convex triangulation, some undesired triangles have been created.

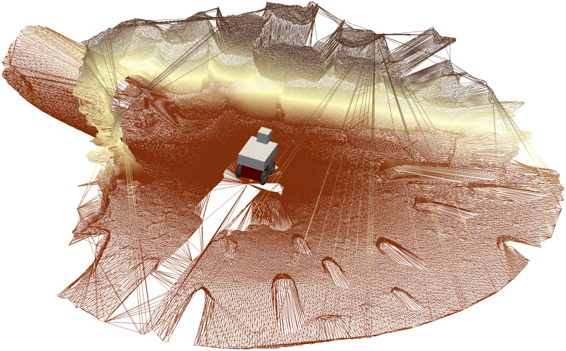

FIG.: Raw Irregular Triangular Mesh (wireframe representation)

Terrain Reconstruction

Three filters are applied to the mesh to remove the shadowed triangles : “perimeter”, “incident angle” and “deep ratio” thresholding.

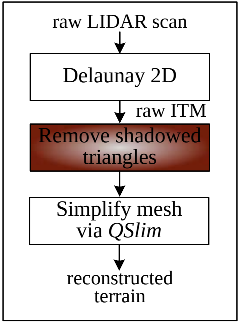

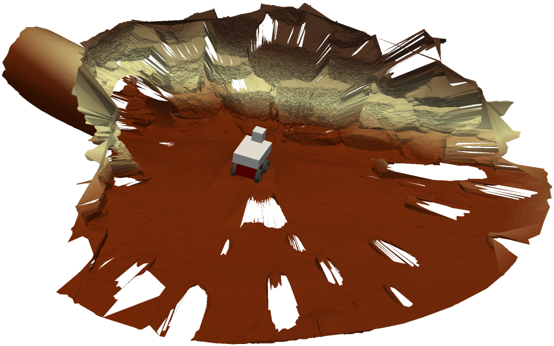

FIG.: Terrain reconstructed (290 000 triangles)

Terrain Reconstruction

The number of triangles is decreased using the mesh simplification algorithm *QSlim*. [Garland, M. and Heckbert, P.S., 1997]

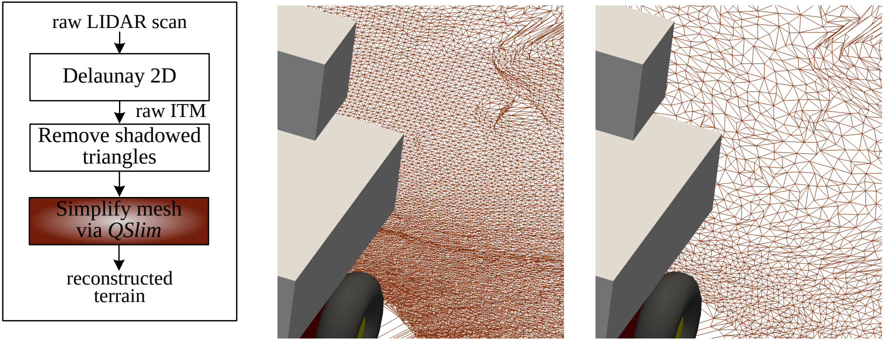

FIG.: Terrain reconstructed and simplified using *QSlim* (290K to 50K tri.)

Navigable Area Extraction

Objective

Extraction of the safe and navigable area from the reconstructed terrain to allow the *point-robot* assumption for the path-planning.

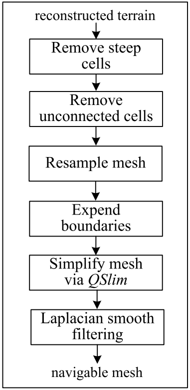

FIG.: Flow diagram of the Navigable Area Extractor (NAE)

Based on the triangle normal vectors, the too steep cells are rejected. The cells unconnected to the ground are also removed.

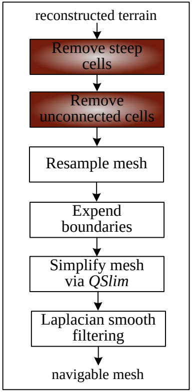

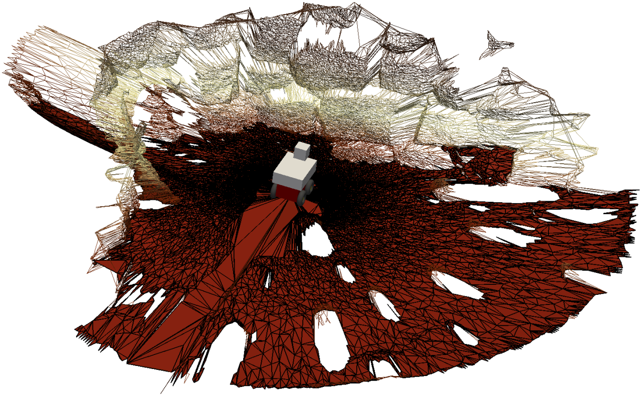

FIG.: Flat area extracted from the reconstructed terrain

Navigable Area Extraction

To correct the varying density of triangles, the mesh is resampled using a linear interpolation approach.

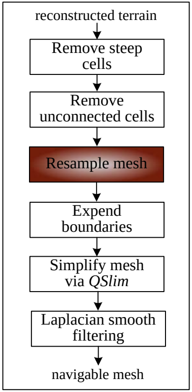

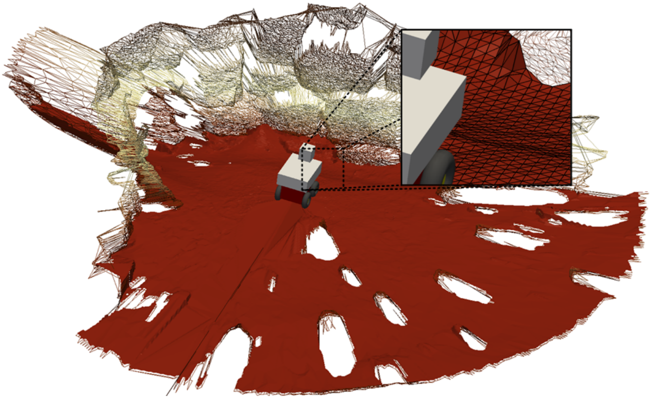

FIG.: Flat area resampled at 5 cm resolution (41k tri.)

Navigable Area Extraction

To take into account the rover dimension, the boundaries are enlarged. This step enables the *point-robot* assumption for the path-planning.

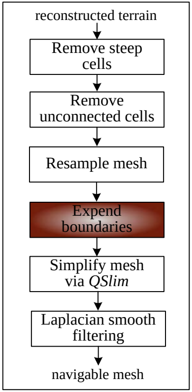

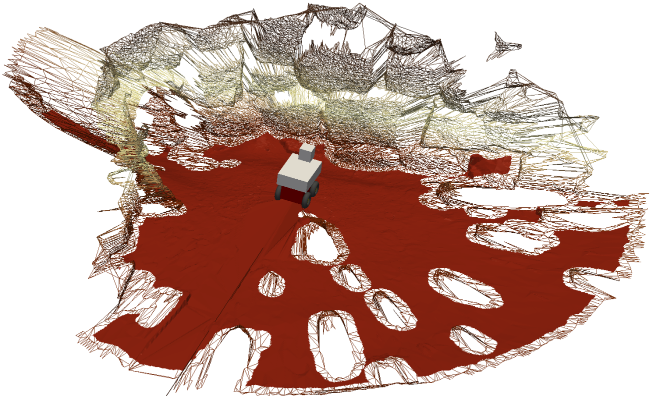

FIG.: Mesh free of obstacle where the boundaries has been enlarged

Navigable Area Extraction

Finally, the mesh is simplified using *QSlim* and filtered via a Laplacian smooth filter to increase the triangles shape.

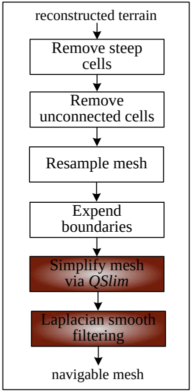

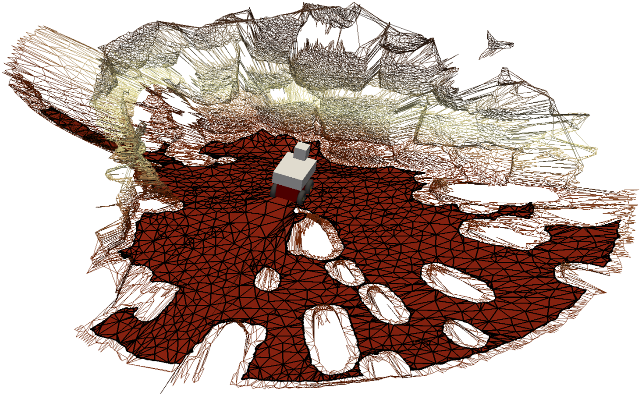

FIG.: Navigable mesh ready for the path-planning (3400 tri.)

Offline Experimental Validation

Objective

To assess the performance and to characterize the processing error and the resulting mesh quality, the CSA NAE has been tested offline using a database containing **688 real LIDAR scans** collected using the CSA testbed during the field testing campaigns of 2007, 2008 and 2009.

- The *root mean square error* introduced by the processing is evaluated using the **approximation of *Hausdorff distance*** between the raw reconstructed terrain and the navigable mesh.
- The overall *mesh quality* is evaluated by the average of each single triangle quality q defined by : $q = \frac{4\sqrt{3}a}{h_1^2+h_2^2+h_3^2}$ [Bank et al, 1990].

Offline Experimental Validation

TAB.: Parameters used by each offline experiment

Parameters	Exp. 1	Exp. 2	Exp. 3
Max. mesh radius (m)	7.0	7.0	7.0
Resampling res. (cm)	7.5	7.5	7.5
Target nb. of cells	**1000**	**4000**	**10 000**
Slope limit (^{o})	25.0	25.0	25.0
Robot radius (cm)	40.0	40.0	40.0

TAB.: CSA NAE average results (data in brackets are standard dev.)

Exp.	Cells nb.	Err. (cm)	Quality	Time (s)
1	870 [110]	1.8 [1.3]	0.65 [0.08]	10.5 [1.0]
2	3770 [410]	0.8 [0.5]	0.83 [0.02]	10.6 [0.9]
3	**9490 [1080]**	**0.5 [0.2]**	**0.87 [0.02]**	**10.8 [0.8]**

Applications of the Navigable Mesh

The navigable mesh can be used to generate a collision-free path using the popular graph-search method $A^\star$.

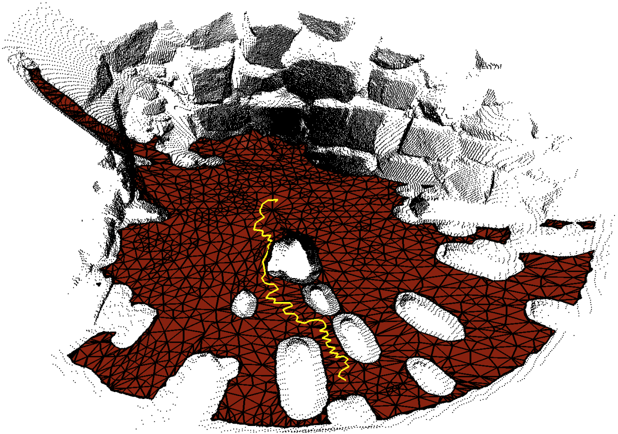

FIG.: Path planned using $A^\star$

Applications of the Navigable Mesh

A smooth collision-free path can also be planned using an approach based on fluid mechanics [Gingras, D. et al., 2010].

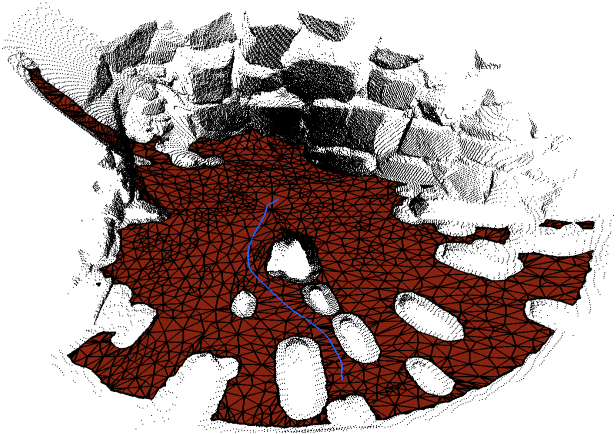

FIG.: Path planned using a fluid mechanics method

Deployment in the Field

The terrain recontruction and the navigable mesh extraction algorithms have been deployed on the CSA Mars Robotics Testbed (MRT) and tested on the CSA Mars Emulation Terrain (MET).

Deployment in the Field

During the 2009 field testing campaign, the approaches have been used 388 times on MET during several autonomous navigations.

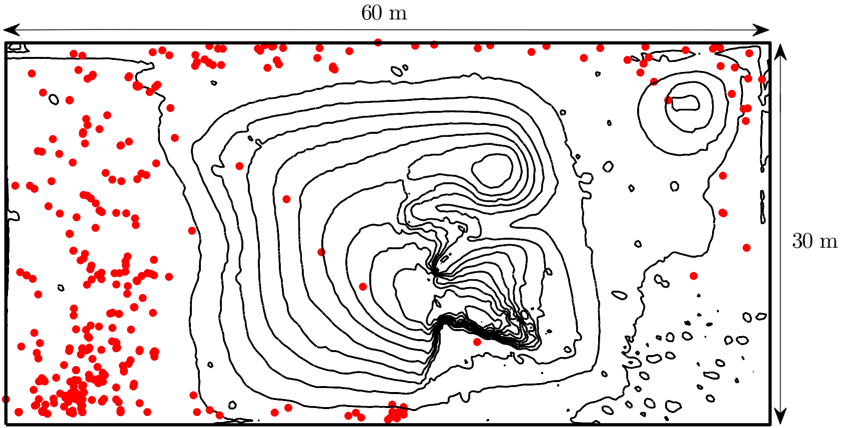

FIG.: Positions on MET where the CSA NAE has been used

Deployment in the Field

(a) Experimental set-up

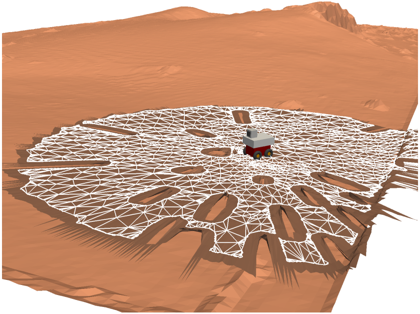

(b) Data collected in the field

FIG.: Example of an extraction of navigable area performed in the field

Deployment in the Field

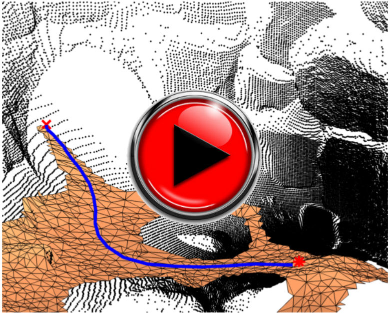

FIG.: Videos presenting an experiment conducted using the CSA testbed

Conclusions

This work presented an approach to model rough terrains by fitting an ITM on point clouds collected using a 360º LIDAR sensor. The reconstructed surface is processed to preserve only the navigable area. The resulting mesh is compact and simplifies the path planning. An experimental validation has been achieved on 688 LIDAR scans collected in the CSA MET. This test has shown that the approach can achieve a data reduction factor up to 93 %, with a reconstruction error of order of 0.5 cm and a good mesh quality. The algorithms have been deployed in a real ground rover and tested 388 times in the field.

Questions

David.Gingras@asc-csa.gc.ca